Journal of Geoscience and Environment Protection, 2020, 8, 139-149
https://www.scirp.org/journal/gep
ISSN Online: 2327-4344
ISSN Print: 2327-4336

Apply X-Ray Fluorescence and γ-Ray Spectroscopy to Analyze Igneous and Sedimentary Environmental Samples of Al-Atawilah (Al-Baha), Saudi Arabia

Bashayer M. Al-Zahrani[1*], Haifa S. Alqannas[2], Safia H. Hamidalddin[2]

[1]Physics Department, Faculty of Science, Al Baha University, Al Baha, Saudi Arabia
[2]Physics Department, Faculty of Science, University of Jeddah, Jeddah, Saudi Arabia
Email: *bmsalzahrani@bu.edu.sa

How to cite this paper: Al-Zahrani, B. M., Alqannas, H. S., & Hamidalddin, S. H. (2020). Apply X-Ray Fluorescence and γ-Ray Spectroscopy to Analyze Igneous and Sedimentary Environmental Samples of Al-Atawilah (Al-Baha), Saudi Arabia. *Journal of Geoscience and Environment Protection, 8,* 139-149.
https://doi.org/10.4236/gep.2020.811008

Received: October 16, 2020
Accepted: November 14, 2020
Published: November 17, 2020

Abstract

Igneous and sedimentary rocks contain an amount of natural radioactivity (NORM). U-238, Th-232 and their decay products, and K-40 are important sources of gamma-radiation. Knowledge of the radionuclide content of rocks is necessary to estimate the exposure of the population to the radiation. Many types of rocks are used in building and industries, thus the radiation detection is important, it provides a baseline map of levels of the radioactivity in the study region. The purpose of this study is to evaluate the activity concentrations of the natural radionuclides (U-238 (Ra-226), Th-232 and K-40) and the fallout nuclide (Cs-137) (if found) in thirty samples of igneous and sedimentary rocks of Al-Atawilah (Al-Baha). The samples were collected and prepared during 2018/2019, and analyzed with a good experimental instrument (High energy resolution γ-ray spectroscopy with HPGe detector), also these rock samples were analyzed with X-ray fluorescence to subdivided these rocks based on the major oxides proportions contained of each sample. The mean activity concentrations of naturally radionuclides were found in the igneous rock samples varied depending on the type of the igneous rock. For sedimentary rock samples, the activity concentrations were found high for quartz sandstone sample, which may be due to its high proportion of SiO_2 and K_2O. The estimated mean values of absorbed dose rate are within the permissible limit value. The findings indicate high dose level values in granite (rhyolite) and most of diorite (andesite) igneous rock samples while gabbro (basalt) igneous rock samples (except for one sample) record low levels of dose rate. All sedimentary rock samples have low dose rate (except for the quartz sandstone sample).

Keywords

Classification of Igneous and Sedimentary Rocks, X-Ray Fluorescence Spectroscopy, Gamma-Ray Spectroscopy, Activity Concentration, Absorbed Dose Rate

1. Introduction

Many of the planets in the Solar System are mainly consist of rocks. Rocks are composed of minerals, both of them are the fundamental of the Earth's crust structure. The rocks have great economic uses, also, many rocks are frequently used decoratively especially crystalline igneous rocks and marble. The defining features of any rock, and thus the means by which it can be recognized and named, are a direct result of how it is formed. Igneous rocks are created when magma or lava crystallizes. Whereas Sedimentary rocks are formed by weathering and erosion of pre-formed rocks, transportation of the grains by the wind or a river system, and finally accumulation in water or on the land (Pellant & Pellant, 2014). The content and the percentage of minerals contained in the rocks are studied by X-Ray Fluorescence (XRF). XRF reports chemical composition to indicate the content and the percentage of element dominate the rock samples and to classify them (Jamaluddin et al., 2018). The distribution of naturally occurring radionuclides depends on the type and origin of rocks and the processes which concentrated them (Bezuidenhout, 2019). Natural radionuclides are over a wide present in environment of the Earth, which is arranged geological formations in Earth's crust (rocks, soil, water plants and air). When the rocks are disintegrated by natural process, the resulting radionuclides are carried to the soil by rain and flows (Olufunmbi et al., 2016; Khan et al., 2018). Ra-226 and its daughter product effects are 98.5% of the radiological of U-238 series, the contribution of Ra-226 is often referred to instead of U-238 (Khandaker et al., 2017). In the present study, the X-ray fluorescence analytical technique was used to analyze igneous and sedimentary rock samples from Al-Atawilah (north of Al-Baha region), and to classify them based on the chemical composition, which is one of the main characteristics of the rocks. Silica (SiO_2) is the vast majority mineral and its proportion is the most useful criteria of rock's classification. The radionuclides activity concentrations of Ra-226, Th-232 and K-40 were determined in rock samples by Gamma-ray spectroscopy system includes hyper-purity germanium (HPGe) detector, and to estimate the doses originate from the existence of the natural radionuclides in the classified rocks.

2. Methods and Materials

2.1. X-Ray Fluorescence Spectroscopy

X-ray fluorescence (XRF) spectroscopy is a non-destructive instrumental technique that enables to determine the chemical composition of a sample based on

the measurements of the intensities and wavelengths of their spectral lines produced by secondary excitation. Figure 1 shows X-ray fluorescence mechanism of an atom. An X-ray primary beam irradiates the sample and excites each chemical element to produce fluorescent (or secondary) X-rays. These emitted X-rays are characteristic of the atom, that give the qualitative analysis of the element. The energy of the emitted X-ray photon is the energy difference between the two levels (initial and final) involved in the electronic transition. The X-ray intensities of an unknown sample are compared to an appropriate standards, this provides quantitative analysis of the element. The measured sample can be of any form, powder, solid, liquid, and manufactured materials (such as wire and rod), etc. (Bertin, 1975; Kalnicky & Singhvi, 2001).

2.2. Gamma-Ray Spectroscopy

The samples have been preparing for the gamma spectrometric measurements as follows:

1) Eighteen igneous rock samples and twelve sedimentary rock samples were collected from Al-Atawilah (20.273351˚N, 41.358325˚E) north of Al-Baha region, southeast of Saudi Arabia (Figure 2).

2) All rocks samples were obtained at depth of 5 cm from the study region. The collected samples were dried, pulverized and then sieved through less than 1mm-mesh size (IAEA, 1989).

3) All crushed sieved rock samples were filled into Marinelli beakers, weighed and hermetically sealed for more than one month, in order to achieve the secular equilibrium between Ra-226 and Th-232 and their progenies (Onjefu et al., 2017; Chowdhury et al., 2020).

The gamma-ray spectroscopy is a rapid and nondestructive analysis used to measure of radionuclides activity concentrations in the rock samples. The detector had resolution of 2 keV at 1332.5 keV of Co-60 and relative efficiency of 25%. The detector is placed in a cylinder heavy lead to lessen the values of radiation background. The lead shield contains an internal concentric of copper to

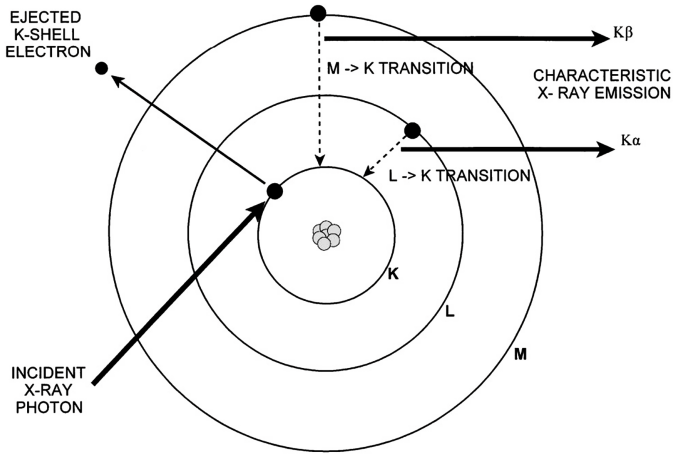

Figure 1. X-ray fluorescence mechanism of an atom (Kalnicky & Singhvi, 2001).

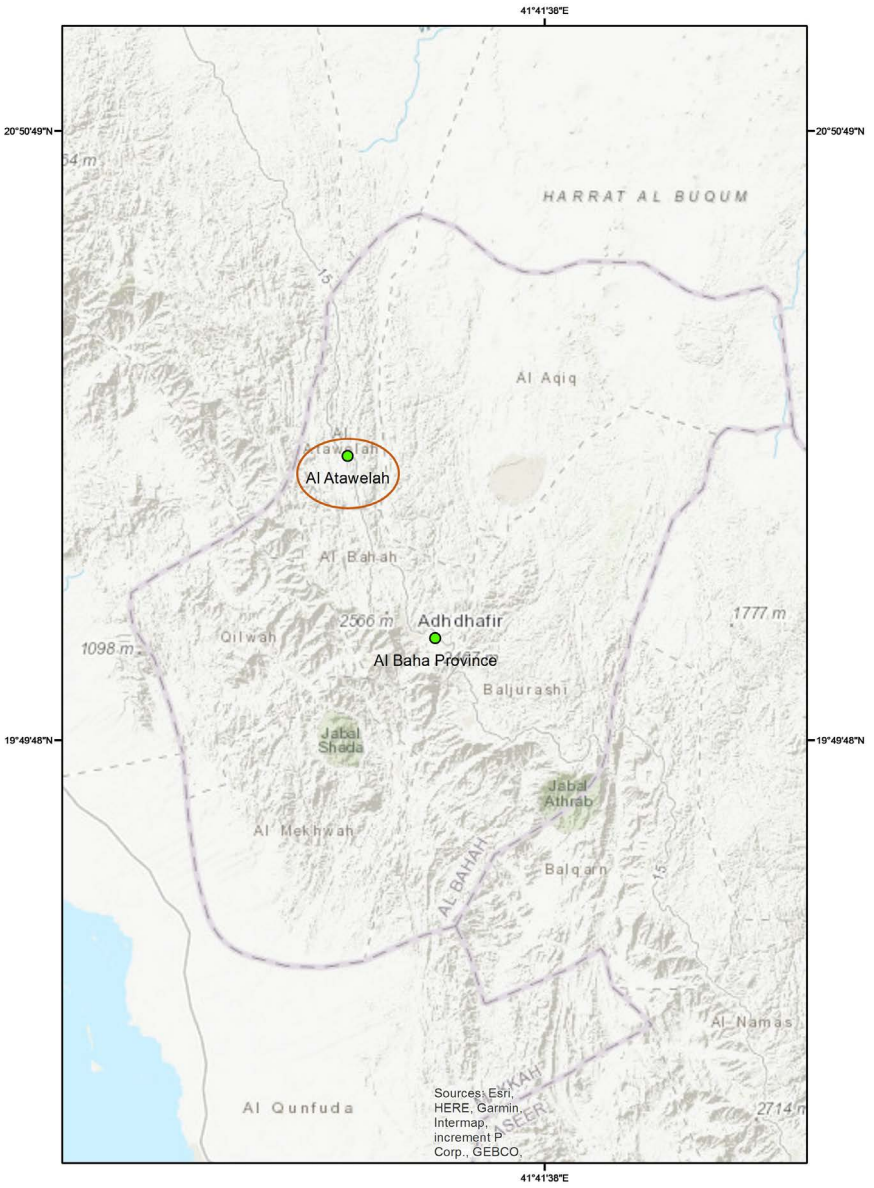

Figure 2. Al-Atawilah location in Al-Baha region.

avoid interference X-rays by lead (Saher et al., 2013; Rosianna et al., 2020). For successful operation of HPGe detector, it is cooled to cryogenic temperature at least 12 hours before making measurements by liquid nitrogen (LN2) of −196˚C = 77˚K.

The activity concentration (A_C) was carried out using the following formula (Al-Zahrani, 2017; Nafee et al., 2017; Al-Zahrani et al., 2020):

$$A_C\left(\mathrm{Bq}\cdot\mathrm{kg}^{-1}\right) = N_C/m\beta\epsilon \tag{1}$$

where N_C is the net count area of the gamma line for the measured sample (counts/second), m is mass of the sample, ϵ is the absolute efficiency of the spectrometer at the photo-peak energy and β is the probability of emission of the gamma ray. The activity concentration of each nuclide is estimated from the

mean concentrations of several energies for the same nuclide or nuclides in the series. Table 1 shows the radionuclides and their energies and branching ratios that used to estimate the activity concentrations of the rock samples under studying.

Absorbed dose rate can be derived from the activity concentrations obtained from the samples. Table 2 shows conversion factors of activity concentration to absorbed dose rate as reported by UNSCEAR, 2000. Thus, the absorbed dose rate (D_R) can be determined by applying the following formula (UNSCEAR, 2000; Onjefu et al., 2017):

$$D_R\left(\text{nGy}\cdot\text{h}^{-1}\right) = 0.462C_{Ra} + 0.604C_{Th} + 0.0417C_K \quad (2)$$

where C_{Ra}, C_{Th} and C_K are respectively the activity concentrations of ^{226}Ra, ^{232}Th and ^{40}K.

3. Results and Discussion

3.1. Classification of the Igneous and Sedimentary Rocks Samples Based on Their Chemical Composition

Rocks are important in mapping of natural resources. Igneous rocks are encountered in geothermal environments. Igneous rocks especially very recent are

Table 1. Radionuclides used for the determination of the activity concentrations.

Parent nuclei	Daughter nuclei	Energy (keV)	Photon/disintegration
^{226}Ra	^{214}Pb	295.09	0.201
		351.87	0.383
	^{214}Bi	609.31	0.499
		1120.27	0.162
		1764.5	0.16
^{232}Th	^{228}Ac	338.42	0.130
		911.16	0.303
		968.97	0.183
	^{212}Pb	238.58	0.437
	^{212}Bi	727.25	0.081
	^{208}Tl	583.1	0.332
		860.4	0.045
^{40}K	^{40}Ar	1460.8	0.105
^{137}Cs	^{137m}Ba	661.66	0.85

Table 2. Conversion factors of activity concentration to absorbed dose rate (UNSCEAR, 2000).

Radionuclide	Conversion factor (nGy·h^{-1}/Bq·kg^{-1})
^{238}U	0.462
^{232}Th	0.604
^{40}K	0.0417

good indicators of volcanism hence heat source for geothermal system to exist. Sedimentary rocks play a major role in reconstruction of earth's history, also important resources for coal and oil can which they be found in sedimentary environments. Geopressured and geothermal systems are hosted in sedimentary terrains (Mibei, 2014).

The igneous and sedimentary rock samples under investigation were classified based on the chemical composition obtained from X-ray fluorescence technique. Silica (SiO_2) is the vast majority mineral and its proportion is the most useful criteria of rock's classification. Table 3 shows the major detected oxides SiO_2, Al_2O_3, Fe_2O_3, TiO_2, CaO, MgO, Na_2O, K_2O, MnO, SO_3 and P_2O_5 in the igneous and sedimentary rocks samples.

Table 3. Proportions of the major oxides in each sample in the igneous and sedimentary rocks samples.

Type of the rock		Sample code	SiO_2	Al_2O_3	Fe_2O_3	TiO_2	CaO	MgO	Na_2O	K_2O	MnO	SO_3	P_2O_5	L.O.I. (1000˚C) %
Igneous Rock	Granite (Rhyolite)	IGN01	72.10	12.52	4.39	0.40	0.53	1.53	3.14	1.46	0.10	<0.05	0.10	3.36
		IGN02	68.30	14.17	5.24	0.38	0.50	3.61	2.52	1.60	0.13	<0.05	0.18	3.22
		IGN03	63.70	14.53	7.06	0.45	3.50	2.23	4.07	0.62	0.14	<0.05	0.20	3.75
		IGN04	61.80	15.43	7.81	0.63	3.54	2.95	3.13	0.88	0.11	<0.05	0.27	3.35
		IGN05	57.90	16.08	10.82	0.45	3.85	3.41	3.93	0.34	0.18	<0.05	0.23	3.96
		IGN06	57.80	17.25	9.92	0.40	7.05	3.07	2.17	0.39	0.16	<0.05	0.20	2.75
	Diorite (Andesite)	IGN07	57.70	17.71	8.26	0.56	7.43	2.69	0.34	1.74	0.22	<0.05	0.42	3.28
		IGN08	57.65	15.56	10.81	0.47	2.05	3.26	1.51	2.03	0.10	<0.05	0.10	7.79
		IGN09	57.50	17.30	9.18	0.56	2.60	2.83	1.27	1.86	0.25	<0.05	0.27	8.26
		IGN10	56.65	15.00	11.50	0.57	2.96	3.83	2.85	1.16	0.17	1.37	0.25	5.45
		IGN11	55.67	18.43	9.74	0.59	1.23	2.96	1.79	3.73	0.17	<0.05	0.16	6.53
		IGN12	54.73	18.60	10.84	0.78	2.88	4.44	1.83	1.81	0.22	<0.05	0.24	4.88
		IGN13	53.49	17.14	12.23	0.41	5.99	5.01	2.22	0.22	0.30	<0.05	0.15	4.22
		IGN14	52.40	17.19	12.23	0.43	7.24	5.49	2.50	0.74	0.22	<0.05	0.23	3.30
	Gabbro (Basalt)	IGN15	52.10	17.72	12.54	0.43	5.89	5.37	2.34	0.74	0.21	<0.05	0.17	4.14
		IGN16	51.47	16.18	13.35	0.55	5.25	5.59	2.08	1.01	0.20	<0.05	0.22	5.43
		IGN17	51.40	15.06	10.65	0.44	8.03	5.94	2.81	0.42	0.16	<0.05	0.20	5.53
		IGN18	51.20	24.82	8.56	0.48	6.03	2.25	2.43	2.15	0.11	<0.05	0.17	2.97
Sedimentary Rock	Quartz sandstone	SED19	76.40	12.59	1.39	0.07	0.09	0.45	2.91	3.97	< 0.05	<0.05	0.04	1.23
	Greywacke	SED20	69.10	14.02	6.31	0.34	0.75	2.62	3.65	0.99	0.21	<0.05	0.14	3.11
	Shale	SED21	61.20	16.51	8.60	0.50	3.38	2.56	4.37	0.84	0.17	<0.05	0.30	3.31
		SED22	60.20	14.19	9.67	0.44	6.50	3.59	1.28	0.45	0.22	<0.05	0.20	3.59
		SED23	59.30	15.91	8.96	0.53	6.05	2.66	2.62	0.49	0.19	<0.05	0.31	3.50
		SED24	57.16	15.02	11.85	0.48	2.45	3.87	1.48	0.78	0.15	<0.05	0.22	8.07
		SED25	56.03	14.93	11.17	0.61	3.51	4.27	3.50	0.71	0.18	<0.05	0.33	6.34
		SED26	54.29	15.68	11.83	0.61	6.08	3.60	2.80	0.09	0.24	<0.05	0.24	5.89
		SED27	48.66	16.44	14.73	0.43	6.89	5.18	3.60	0.12	0.28	<0.05	0.08	5.23
		SED28	47.45	17.70	14.47	0.55	9.02	5.13	0.90	0.25	0.30	<0.05	0.30	5.65
		SED29	44.92	14.14	17.97	1.43	5.77	7.94	1.05	0.36	0.47	<0.05	0.25	7.67
		SED30	44.86	17.52	14.93	0.89	8.02	4.73	0.94	0.55	0.40	<0.05	0.33	8.81

1) Acid rocks (rhyolite & granite) are rich in SiO_2 (over 65%), samples IGN01 and IGN02.

2) Intermediate rocks (andesite & diorite) have between 55% and 65% of SiO_2, samples (IGN03-IGN12).

3) Basic rocks (basalt & gabbro) contain proportion of SiO_2 from 45% to 55%, samples (IGN13-IGN18) (Pellant & Pellant, 2014).

The sedimentary rock samples (SED19-SED30) can be classified according to the SiO_2 proportion as follows (Gray et al., 2014):

1) Quartz sand stone: contains about 78.33% of silica, sample SED19.

2) Greywacke: has about 66.06% of silica, sample SED20.

3) Shale: contain less than 60.28% of silica samples (SED21-SED30).

Sedimentary rocks form up to 66% of the earth's crust. They consider the most of the rocks on the earth's surface and are mainly found on the ocean floor basins which accounts to 70% of total area of the earth. Igneous rocks form the majority of 34% (Ehlers and Blatt, 1997). Also, the igneous and sedimentary rocks are classified based on chemistry and minerals, environment of formation and how they are formed.

3.2. Activity Concentrations

The activity concentrations of the rock samples under studying were tabulated in Table 4, the following findings can be recorded:

1) ^{226}Ra activity concentration values of all igneous rock samples are less than the world average (50 $Bq \cdot kg^{-1}$). Also, ^{226}Ra activity concentration values of sedimentary rock samples (except for quartz sandstone sample (SED19)) are less than the world average (50 $Bq \cdot kg^{-1}$) recommended by UNSCEAR, 2008.

2) ^{232}Th activity concentrations in rhyolite (granite) samples and diorite (andesite) samples are mostly higher than that in gabbro (basalt) samples. All the activity concentrations of ^{232}Th in the igneous rock samples are under the world average (50 $Bq \cdot kg^{-1}$) recommended by UNSCEAR, 2008. All the values of ^{232}Th activity concentration in the sedimentary rock samples (greywacke and shale) are under the acceptable value except for a slight increase in the quartz sandstone sample (SED19). The mean value of ^{232}Th in sedimentary rock samples (12.04) is under the recommended value (50 $Bq \cdot kg^{-1}$) reported in UNSCEAR, 2008.

3) ^{40}K activity concentration values are varied in all igneous rock samples. All the igneous rock samples have ^{40}K activity concentration higher than recommended value, except for diorite (andesite) sample (IGN05) and gabbro (basalt) sample (IGN13). ^{40}K activity concentration values are measured higher than the acceptable value in all the sedimentary rock samples in this study except for (SED26, SED27, SED28 and SED29) shale samples. The calculated mean values of ^{40}K in the igneous and sedimentary rock samples are higher than the recommended value reported in UNSCEAR, 2008 (500 $Bq \cdot kg^{-1}$).

4) The fallout radionuclide (^{137}Cs) is found in the most samples rocks under

Table 4. Activity concentrations of ^{226}Ra, ^{232}Th, ^{40}K and ^{137}Cs, and absorbed dose rate.

Rock type		Sample code	Activity Concentration ($Bq \cdot kg^{-1}$)[a]				Absorbed dose ($nGy \cdot h^{-1}$)[a]
			^{226}Ra	^{232}Th	^{40}K	^{137}Cs	
Igneous Rocks	Granite (Rhyolite)	IGN01	9.56 ± 1.15	8.36 ± 1.66	2100.30 ± 25.40	ND[b]	97.05
		IGN02	12.00 ± 1.26	18.00 ± 2.84	2400.40 ± 26.50	3.62 ± 0.78	116.45
		IGN03	12.00 ± 2.35	10.68 ± 1.45	867.45 ± 19.10	2.40 ± 0.54	48.03
		IGN04	11.50 ± 1.25	14.13 ± 2.25	1240.50 ± 21.40	ND	65.57
		IGN05	10.07 ± 1.34	8.83 ± 2.70	445.70 ± 16.50	1.50 ± 0.40	28.57
		IGN06	11.60 ± 1.11	11.50 ± 1.50	575.46 ± 17.07	4.00 ± 0.58	36.30
	Diorite (Andesite)	IGN07	16.05 ± 1.40	19.10 ± 3.00	2510.00 ± 27.10	3.48 ± 0.72	123.63
		IGN08	17.50 ± 1.42	8.30 ± 1.67	2895.17 ± 28.30	ND	133.83
		IGN09	17.00 ± 1.58	19.83 ± 2.00	2696.45 ± 27.80	ND	132.27
		IGN10	5.86 ± 1.25	9.32 ± 2.45	1589.32 ± 22.83	ND	74.61
		IGN11	13.10 ± 1.48	14.00 ± 2.00	4854.00 ± 35.00	ND	216.86
		IGN12	15.60 ± 1.46	21.42 ± 1.82	2266.58 ± 26.20	2.44 ± 0.60	114.65
	Gabbro (Basalt)	IGN13	6.88 ± 1.13	7.26 ± 1.83	328.08 ± 15.60	ND	21.25
		IGN14	8.27 ± 1.00	5.12 ± 1.01	1021.56 ± 20.30	5.63 ± 0.63	49.50
		IGN15	9.25 ± 1.34	9.00 ± 1.55	1066.17 ± 20.50	0.93 ± 0.40	54.16
		IGN16	7.53 ± 1.27	7.76 ± 2.10	1297.30 ± 21.27	0.90 ± 0.43	62.26
		IGN17	6.53 ± 1.10	8.31 ± 1.41	600.00 ± 17.27	1.60 ± 0.53	33.05
		IGN18	6.18 ± 1.36	6.14 ± 2.40	3154.70 ± 29.43	ND	138.12
	Range		5.86 - 17.50	5.12 - 21.42	328.08 - 4854.00	0.90 - 5.63	28.57 - 216.86
	Average		11.00	11.50	1172.71	1.47	86.00
Sedimentary Rocks	Quartz sandstone	SED19	54.85 ± 2.10	61.26 ± 6.38	6070.75 ± 39.50	ND	315.50
	Greywacke	SED20	7.65 ± 1.12	9.48 ± 1.16	1366.27 ± 21.60	4.00 ± 0.62	66.24
	Shale	SED21	10.00 ± 1.13	8.00 ± 1.55	1216.20 ± 20.70	2.87 ± 0.60	60.13
		SED22	6.00 ± 1.23	7.47 ± 1.05	664.68 ± 17.30	2.34 ± 0.57	35.00
		SED23	10.67 ± 1.35	11.36 ± 1.34	644.40 ± 17.70	ND	38.66
		SED24	10.20 ± 1.30	10.55 ± 1.46	964.78 ± 19.60	2.30 ± 0.55	51.33
		SED25	7.78 ± 1.37	7.12 ± 1.16	968.84 ± 19.30	ND	48.30
		SED26	8.58 ± 1.10	10.71 ± 2.14	110.00 ± 13.00	0.84 ± 0.35	15.02
		SED27	5.58 ± 1.34	5.15 ± 1.33	136.26 ± 14.80	2.00 ± 0.57	11.37
		SED28	8.03 ± 1.27	7.90 ± 1.43	340.25 ± 15.53	1.30 ± 0.47	22.66
		SED29	5.23 ± 1.08	7.38 ± 1.82	401.08 ± 16.30	1.95 ± 0.53	23.60
		SED30	10.00 ± 1.06	11.86 ± 1.55	693.07 ± 18.50	1.57 ± 0.46	40.67
	Range		5.23 - 54.85	5.15 - 61.26	110.00 - 6070.75	0.84 - 4.00	11.37 - 315.50
	Average		12.04	13.18	1131.36	1.60	60.70
(UNSCEAR, 2008)			50	50	500		84

a. The results of the activity concentration and absorbed dose rate were reported in the reference (Al-Zahrani et al., 2020); b. ND: not determined.

investigation. The calculated mean values of ^{137}Cs do not represent any radiologically important.

From the results of gamma-ray spectroscopy and X-ray fluorescence analysis techniques of the igneous and sedimentary rocks, it can be noted that the rock samples that have the lowest proportion of K_2O reflect the lowest activity concentration of ^{40}K (IGN13 in the igneous rock samples and SED26 in the sedimentary rock samples), similarly, highest ^{40}K concentration in the rock samples attributed by highest K_2O in these rock samples (IGN11 in the igneous rock samples and SED19 in the sedimentary rock samples).

3.3. Absorbed Dose Rate

Absorbed dose rate values for rock samples were shown in **Table 4**, and the following observations can be indicated:

1) In the igneous rock samples, the highest value of the absorbed dose rate was found in the granite (rhyolite) samples (IGN01 & IGN02), the diorite (andesite) samples (IGN07, IGN08, IGN09, IGN11, IGN12) and the gabbro (basalt) sample (IGN18). The calculated mean value of the absorbed dose was found within the population-weighted value of 84 $nGy \cdot h^{-1}$ suggested by UNSCEAR, 2008. The range of the total absorbed dose rate of the igneous rock samples is approximately within the typical variety (10 - 200 $nGy \cdot h^{-1}$) (Al-Zahrani, 2017).

2) All values of the absorbed dose rate in the sedimentary rock samples was found less than acceptable value except for that in sample (SED19). The calculated average value of the total absorbed dose is within the acceptable value of 84 $nGy \cdot h^{-1}$ reported by UNSCEAR, 2008.

4. Conclusion

The results of chemical analysis employing X-ray fluorescence spectroscopy show the major oxides proportions of the samples under studying. The igneous and sedimentary rock samples were subdivided based on the major oxides proportions contained in each sample. Naturally occurring radionuclides were determined for eighteen igneous rock samples and twelve sedimentary rock samples using hyper-purity germanium (HPGe) detector. In the igneous rock samples, most gabbro (basalt) samples were recorded the lowest values of activities, while granite (rhyolite) and diorite (andesite) samples varied in the values of activities. Quartz sandstone sample had the highest activity concentrations in the sedimentary rock samples, this may due to the high proportion of SiO_2 and K_2O were contained by this sample. Greywacke sample recorded concentration of ^{40}K higher than shale samples, while ^{226}Ra and ^{232}Th varied in the greywacke and shale samples. Fallout nuclide (^{137}Cs) were found in the most rocks samples under investigated, the low mean values of ^{137}Cs are not of radiologically important. The findings indicate the high dose rate in the granite (rhyolite) samples and most diorite (andesite) samples, therefore it is recommended to limit their usage in building materials and other uses, while the dose rate levels were low in all

gabbro (basalt) samples (except for one sample), thus they are safe to use as well as all sedimentary rocks samples reported low values of the dose rate values (except for the quartz sandstone sample). The results of this study will help to explain the distribution of natural radionuclides in different rocks types of Al-Baha region.

Acknowledgements

We would like to thank the people in Saudi Geological Survey (SGS) who helped us in X-ray fluorescence analysis.

Conflicts of Interest

The authors declare no conflicts of interest regarding the publication of this paper.

References

Al-Zahrani, B. M., Alqannas, H. S., & Hamidalddin, S. H. (2020). Study and Simulated the Natural Radioactivity (NORM) U-238, Th-232 and K-40 of Igneous and Sedimentary Rocks of Al-Atawilah (Al-Baha) in Saudi Arabia. *World Journal of Nuclear Science and Technology, 10,* 171-181. https://doi.org/10.4236/wjnst.2020.104015

Al-Zahrani, J. (2017). Estimation of Natural Radioactivity in Local and Imported Polished Granite Used as Building Materials in Saudi Arabia. *Journal of Radiation Research and Applied Sciences, 10,* 241-245. https://doi.org/10.1016/j.jrras.2017.05.001

Bertin, E. P. (1975). *Principles and Practice of X-Ray Spectrometric Analysis*. New York: Plenum Press. https://doi.org/10.1007/978-1-4613-4416-2

Bezuidenhout, J. (2019). The Relationship among Naturally Occurring Radionuclides, Geology, and Geography: Tsodilo Hills, Botswana. *Journal of Radiation Research and Applied Sciences, 12,* 93-100. https://doi.org/10.1080/16878507.2019.1593717

Chowdhury, C. R., Khijmatgar, S., Chowdhury, A., Kumari, D., Lynch, E., & Gootveld, M. (2020). Radionuclide Activity Concentration in Soil, Granites and Water in a Fluorosis Endemic Area of India: An Oral Health Perspective. *Journal of Oral Biology and Craniofacial Research, 10,* 259-262. https://doi.org/10.1016/j.jobcr.2020.05.003

Ehlers, G. E., & Blatt, H. (1997). *Petrology, Igneous Sedimentary and Metamorphic*. New Delhi: CBS Publishers and Distribution.

Gray, J. M., Bishop, T. F. A., & Wilford, J. R. (2014). Lithology as a Powerful Covariate in Digital Soil Mapping. In *GlobalSoilMap: Basis of the Global Soil Information System* (pp. 433-439). Leiden: CRC Press/Balkema. https://doi.org/10.1201/b16500-78

IAEA, I. (1989). *Measurement of Radionuclides in Food and the Environment*. Wien: International Atomic Energy Agency, Technical Report Series No. 295.

Jamaluddin, Darwis, A., & Massinai, M. A. (2018). X-Ray Fluorescence (XRF) to Identify Chemical Analysis of Minerals in Buton Island, SE Sulawesi, Indonesia. *IOP Conference Series: Earth and Environmental Science, 118,* Article ID: 012070. https://doi.org/10.1088/1755-1315/118/1/012070

Kalnicky, D. J., & Singhvi, R. (2001). Field Portable XRF Analysis of Environmental Samples. *Journal of Hazardous Material, 83,* 93-122. https://doi.org/10.1016/S0304-3894(00)00330-7

Khan, A. R., Mir, A. A., Saeed, S., Rafique, M., Asim, K. M., Iqbal, T., Rahman, S. U. et al. (2018). Classification of Rocks Radionuclide Data Using Machine Learning Techniques. *Acta Geophysica, 66,* 1073-1079. https://doi.org/10.1007/s11600-018-0190-6

Khandaker, M. U., Nasir, N. L. M., Zakirin, N. S., Kassim, H. A., Asaduzzaman, K., Bradley, D. A., Hayyan, A. et al. (2017). Radiation Dose to the Malaysian Populace via the Consumption of Bottled Mineral Water. *Radiation Physics and Chemistry, 140,* 173-179. https://doi.org/10.1016/j.radphyschem.2017.01.018

Mibei, G. (2014). *Introduction to Types and Classification of Rocks.* Geothermal Development Company, 1374011.

Nafee, S. S., Al-Othmany, D., Hamidalddin, S. H., Al-Zahrani, J., Alharbi, W., & Barashed, H. M. (2017). Measurement of Gamma Emitting Radionuclide for Assessment Environmental Hazards of Radiation in Rock and Soil Samples of Shabwah and Hadramout Regions, Yemen. *Journal of Geoscience and Environment Protection, 5,* 66-75. https://doi.org/10.4236/gep.2017.55005

Olufunmbi, A., Akinjide, O., Moromoke, O., & Oluwafunmito, O. (2016). The Concentration of Natural Radionuclides in Soil Samples from the Practical Year Agricultural Farmland, University of Ibadan. *Journal of Applied Physics, 8,* 60-68. https://doi.org/10.9790/4861-0804036068

Onjefu, S. A., Taole, S. H., Kgabi, N. A., Grant, C., & Antoine, J. (2017). Assessment of Natural Radionuclide Distribution in Shore Sediment Samples Collected from the North Dune Beach, Henties Bay, Namibia. *Journal of Radiation Research and Applied Sciences, 10,* 301-306. https://doi.org/10.1016/j.jrras.2017.07.003

Pellant, C., & Pellant, H. (2014). *Rocks and Mineral*. London: Bloomsbury Publishing.

Rosianna, I., Nugraha, E. D., Syaeful, H., Putra, S., Hosoda, M., Akata, N., & Tokonami, S. (2020). Natural Radioactivity of Laterite and Volcanic Rock Sample for Radioactive Mineral Exploration in Mamuju, Indonesia. *Geosciences, 10,* 376. https://doi.org/10.3390/geosciences10090376

Saher, M. D., Samia, M. E. B., Amany, T. S., & Najat, F. A. (2013). Natural Radioactivity Assessment and Radiological Hazards in Soils from Qarun Lake and Wadi El Rayan in Faiyum, Egypt. *Open Journal of Soil Science, 3,* 289-296. https://doi.org/10.4236/ojss.2013.37034

United Nations Scientific Committee on the Effects of Atomic Radiation (UNSCEAR) (2000). *UNSCEAR 2000 Report to the General Assembly, with Scientific Annexes*. New York: UNSCEAR.

United Nations Scientific Committee on the Effects of Atomic Radiation (UNSCEAR) (2008). *UNSCEAR 2008 Report to the General Assembly, with Scientific Annexes*. New York: UNSCEAR.